Defense Technical Information Center Compilation Part Notice

ADP012651

TITLE: Continuous and Time Resolved Optically Detected Magnetic Resonance Studies of InP Nanoparticles

DISTRIBUTION: Approved for public release, distribution unlimited

This paper is part of the following report:

TITLE: Progress in Semiconductor Materials for Optoelectronic Applications Symposium held in Boston, Massachusetts on November 26-29, 2001.

To order the complete compilation report, use: ADA405047

The component part is provided here to allow users access to individually authored sections of proceedings, annals, symposia, etc. However, the component should be considered within the context of the overall compilation report and not as a stand-alone technical report.

The following component part numbers comprise the compilation report:
ADP012585 thru ADP012685

Mat. Res. Soc. Symp. Proc. Vol. 692 © 2002 Materials Research Society H9.23

Continuous and Time Resolved Optically Detected Magnetic Resonance Studies of InP Nanoparticles

L. Langof, E. Ehrenfreund, and E. Lifshitz
Solid State Institute, Technion – Israel Institute of Technology, Haifa 32000, Israel
O. I. Micic and A. J. Nozik
National Renewable Energy Laboratory, Golden, Colorado 80401, USA

ABSTRACT

Carriers in small colloidal InP nanoparticles are in strong quantum confinement regime. The low temperature photoluminescence spectrum of InP nanoparticles is composed of an excitonic luminescence at high energies and a non-excitonic defect emission band at lower energies. HF etching of the nanoparticles reduces the defect emission and enhances the exciton process.

In this work we apply optically detected magnetic resonance spectroscopy (ODMR) both in continuous wave and time resolved mode (TR-ODMR) to study the defect luminescence in InP nanoparticles. The results show that the defect luminescence originates from weakly coupled electron-hole pair, where the electron is trapped at the surface by phosphorous vacancy, Vp, and the hole is located at the valence band. Additionally, the results suggest that the non-etched samples are dominated by Vp at the surface. Those are mainly eliminated upon HF treatment, leaving behind small percent of Vp in the core of the nanoparticle. We also find the electron-hole exchange interaction from circular polarized ODMR measurements. The TR-ODMR measurement further clarifies the spin dynamics and characteristic of the magnetic sites. Fitting these measurements to the simulated response of the PL intensity to the square wave modulated microwave power revealed that the spin relaxation time and radiative lifetime of electron-hole pair in the nanoparticles are in the microseconds regime.

INTRODUCTION

In recent years, there has been an increase of interest in the scientific and technological aspects of colloidal semiconductor nanoparticles (NPs). These materials exhibit unique chemical and physical properties, differing substantially from those of the corresponding bulk solids. The special properties are associated with the quantum size effect and the control of surface quality. The impact of the quantum size effect in the III-V NPs is of a special interest, due to their large exciton Bohr radius (10-34 nm) and relatively narrow band gap (0.4-1.5 eV). In such a case, the Bohr radius exceeds the NP diameter, which in turn leads to strong confinement of carriers and a relatively large blue shift of the band edge.

Although carrier confinement in colloidal III-V NPs is expected to lead to enhanced PL efficiency, this is not frequently observed, presumably due to the trapping of carriers at the surface and non-radiative recombination. Indeed, Micic *et al.* [1] showed that the growth of InP colloidal NPs under excess indium produces a red luminescence band, while the growth under excess phosphorous eliminates this band. Furthermore, etching of the samples with HF partially quenches the red luminescence from surface traps. This suggests that the red band corresponds to stoichiometric defects at the surface. Thus, the ultimate goal of this work is concerned with

the identification of the surface trapping sites and their influence on the recombination processes.

EXPERIMENTAL DETAILS

Colloidal InP NPs, capped with organic ligands were prepared by wet chemical methods, while their surfaces were treated by several etching procedures. An indium chloride ($InCl_3$) and tris-(trimethyl-silyl)phosphine ($P(SiMe_3)_3$) were used as the starting reactants. A detailed description of the preparation procedure is given in reference [2].

In the continuous wave (cw) ODMR experiment, we monitored a change in luminescence intensity, ΔI_{PL}, resulting from a magnetic resonance event at the excited state. Thus, a plot of ΔI_{PL} versus the strength of an applied external magnetic field (B), during a simultaneous application of a microwave (MW) radiation, led to an electron spin resonance-like spectrum The emitted beam was detected in either of the following directions: (a) parallel to the external magnetic field (Faraday configuration), or (b) perpendicular to it (Voight configuration). A total emission or a circular-polarization component (σ^+ or σ^-) was detected in both configurations. Detailed description of the cw and TR ODMR setup is given elsewhere [3].

The time-resolved ODMR (TR-ODMR) signal is a luminescence response to a microwave pulse under the resonance magnetic field.

RESULTS

The photoluminescence (PL) spectra of HF etched and non-etched InP NPs (with average diameter of 4.4 nm) at 1.4K are shown by the dashed lines in Figure 1(a) and 1(b), respectively. The PL spectrum of the etched sample is dominated by an exciton band centered at ~2 eV, and accompanied by a weak tail at the low energy side. On the contrary, the non-etched sample is

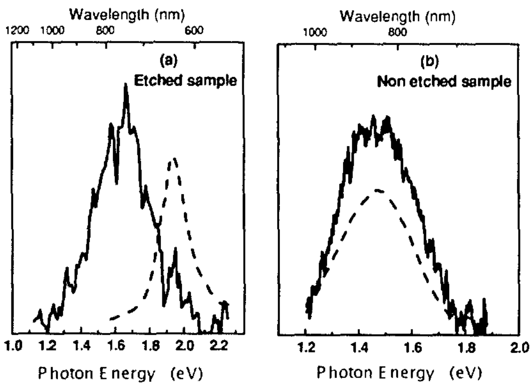

Figure 1. The photoluminescence spectra of non-etched and HF etched InP NPs (dashed line), and spectrally dependent ODMR spectra (solid line).

dominated by a deep broad band centered at 1.5 eV, with a full width half maximum (FWHM) of 0.2 eV, and a weak exciton shoulder at 1.8 eV. It should be noted that the etching process strips one or two monolayers of InP from the external surface, which reduces the NPs size and leads to a shift of the exciton band. The ODMR spectral dependence curves of both samples are shown in Figure 1 by the solid lines. They were recorded by measuring the change in PL intensity versus emission energy during an application of the resonance conditions, with an external magnetic field of 0.4 Tesla and MW radiation of υ_{MW}=10.8 GHz. Both samples showed a spectral dependent ODMR band, which ranged between 1.2-2.0 eV, covering the entire non-exciton regime. In fact, this spectral dependence solely coincides with the PL spectrum of the non-etched sample, but deviates from the exciton band of the etched sample.

Representative cw ODMR spectra of the non-etched sample, recorded with circular polarizer in Faraday and Voight configurations, are shown in Figures 2(a) and 2(b), respectively. The σ^+ and σ^- detection in the Faraday configuration showed similar resonant bands, however they were shifted one with respect to the other by about 0.008 Tesla. However, the circular polarized components are indistinguishable in the Voight configuration.

The TR-ODMR spectrum of the non-etched sample, obtained with a MW transient measurement, is shown in Figure 3 by the noisy line. The solid line corresponds to a theoretical fit (*vide infra*), while the corresponding MW pulse is shown below the spectrum. This spectrum shows an instant spike of the luminescence intensity at the rising edge of the MW pulse, followed by an intensity decay, then by a sudden negative drop at the falling edge of the MW pulse, and finally, by a recovery to a steady state intensity. The spin dynamics associated with this sequence of changes will be given in the Discussion.

DISCUSSION

The PL of the etched sample is characterized by an exciton luminescence, accompanied by a tail, presumably associated with a stoichiometric defect recombination. Chemical treatment of

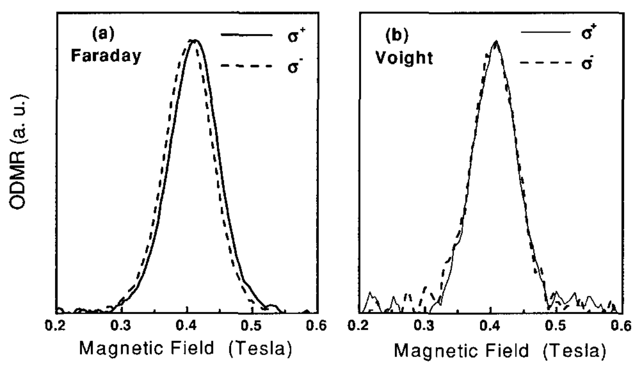

Figure 2. ODMR spectra of the non-etched sample, recorded with the circular polarizer in Faraday (a) and Voight (b) configurations.

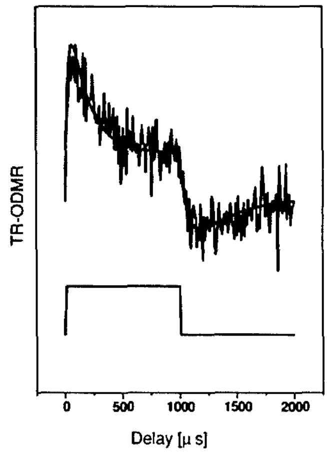

Figure 3. The TR-ODMR spectrum of non-etched sample, obtained with a MW transient measurement.

the samples with excess phosphorous during the growth or post HF etching reduces the tail recombination and enhances the exciton efficiency. Indeed, the defect recombination band dominates the PL of non-etched sample. The ODMR spectral dependence coincides solely with the defect luminescence band and thus, the magnetic resonance phenomena discussed below determine the nature of this recombination (trap-to-trap or trap-to-band), chemical identification of a defect site, electron-hole (e-h) exchange interaction and the spin dynamics.

The experimental ODMR spectra showed the existence of a single positive band, both in the Faraday and Voight configurations, which could be fitted to a single Gaussian function. Furthermore, both the left and right circularly detected ODMR spectra are positive, but mutually shifted by about 0.008 Tesla in the Faraday configuration. This is in contradiction with the anticipation of two independent resonance bands for weakly coupled electron and hole, or a creation of a bound exciton with a negative band in the Voight configuration [3]. Instead, the experimental evidence supports the occurrence of magnetic resonance transitions, associated with trapped electron (F_e=1/2) and a valence hole (F_h=3/2) spin system. Considering a sole spin flipping of electrons, the ODMR band could be fitted to a theoretical curve calculated by a use of conventional spin Hamiltonian including Zeeman splitting, electron hole exchange interaction J, and hyperfine interaction with the surrounding nuclei. We used g_e=1.93 and J= 0.28μeV for a non-etched sample, and g_e=1.98 for an etched sample. The increase in the g factor in the etched sample may arise from a confinement effect, due to the reduction of the NPs size upon etching or due to the existence of a different crystallographic defect. The J value was derived from the mutual shift of the σ^+ and σ^- spectra shown in Figure 2(a).

The extended wave function of the valence hole enabled a reasonable overlap with the trapped electron and indeed an e-h exchange interaction deviate from the exchange value of an exciton (30 meV) and resemble the value which was found recently for trapped electron-trapped hole recombination (0.2 μeV) in colloidal NPs [4].The magnitude of the exchange interaction is proportional to the overlap integral of the wave function of both carriers and is given by:

$$J = J_0 \exp(-2r/r_0) \quad (1)$$

where r_0 is the Bohr radius of the wave function of the less localized carrier and r is the exciton radius. It is reasonable to assume that r is close to the radius of the NPs and thus, may deviate from a single value due to the existence of a ~10% distribution in the NPs size.

The g_e value of the electron deviates considerably from that of a reported bulk value of g_e=1.15-1.5 at the conduction band, however, it does not approach the free electron g_e=2.0. This suggests that the electron is trapped at a phosphorous vacancy, but is slightly delocalized over the first next indium neighbors. The experimental lineshape could be simulated only by addition of hyperfine interactions between the trapped electron with the surrounding indium nuclei. The indium atom has a nuclear spin of I=9/2 with neutral abundance of 100%, while a hyperfine interaction with n next neighbors should lead to 2nI+1 subbands. However, since the indium isotropic hyperfine constant is 390MHz [5], and the sample is studied as a powder, the detailed hyperfine lines cannot be resolved and instead, this coupling contributes to the broadening of the studied resonance band.

The time-resolved ODMR measurement further clarifies the spin dynamics and characteristics of the magnetic sites (radiative versus non-radiative). Assuming that saturation of the spin levels is avoided, the spin kinetic processes of the |+3/2, -1/2 > and |+3/2, +1/2 >, or |-3/2, -1/2 > and |-3/2, +1/2 > pair states are given by the following equations:

$$\begin{aligned}
\frac{dn_1}{dt} &= -\frac{n_1}{\tau_1} + G - \frac{n_1 - (n_1 + n_2)(1-\rho)}{T_1} - (n_1 - n_2)P_{MW} \\
\frac{dn_2}{dt} &= -\frac{n_2}{\tau_2} + G - \frac{n_2 - (n_1 + n_2)\rho}{T_1} - (n_2 - n_1)P_{MW} \\
\rho &= \frac{1}{1+\exp(\Delta E/kT)} \quad , \quad \Delta E = h\nu_{MW}
\end{aligned} \quad (2)$$

n_1 and n_2 correspond to the population of single pair states. G corresponds to the generation rate, while τ_1 and τ_2 are the corresponding decay times (when $\tau^{-1} = \tau_{rad}^{-1} + \tau_{nrad}^{-1}$, rad and nrad correspond to the radiative and non-radiative processes). T_1 is the spin-lattice relaxation, while P_{MW} corresponds to the MW power. exp(-E/kT) is the occupancy probability in thermal equilibrium. The analytical solution of four kinetic equations (with $P_{MW}=0$ and $P_{MW}\neq 0$) yields a theoretical change in the PL intensity due to a magnetic resonance between two states, induced by a square-wave modulation of the MW power. The experimental TR-ODMR spectrum was simulated with τ_{rad1}=100 µsec, $\tau_{nrad1/2}$=800 µsec, $\tau_{rad2} >> \tau_{rad1}$, and T_1=250 µsec, as shown by the solid smooth line in figure 3. This simulation suggests that the defect-to-band recombination is a radiative process, involving trapping of an electron at a phosphorous vacancy.

CONCLUSIONS

InP NPs prepared by colloidal techniques were investigated. The research was focused on the characterization of a defect luminescence band. cw and TR-ODMR spectroscopy was utilized in combination with conventional luminescence technique. The ODMR spectrum consists of a single broad positive resonance composed of left and right circular polarized components, mutually shifted by 0.008 Tesla in a Faraday configuration. The defect luminescence was

identified as a recombination of a valence band hole, with total angular momentum of 3/2, and an electron trapped at a Vp site, with total angular momentum of 1/2. The non-etched samples are dominated by Vp sites at the surface, while the etched samples are left with a small percent of vacancies at the core. The TR-ODMR measurements revealed characteristic decay times of about 100μs for the radiative and about 800μs for nonradiative spin levels. This measurement also revealed that a spin-lattice relaxation is about 250μs.

REFERENCES

1. D. Bertram, O. Micic and A. Nozik, Phys. Rev. B **57,** R4265 (1998).
2. O. I. Micic, K. M. Jones, A. Cahill and A. J. Nozik, J. Phys. Chem. B **102,** 9791 (1998).
3. L. Langof, E. Ehrenfreund, E. Lifshitz, O.I. Micic, and A. J. Nozik, in press, J. Phys. Chem.
4 E. Lifshitz, A. Glozman, I. D. Litvin, and H. Porteanu, J. Phys. Chem. B **104**, 10449 (2000).
5. H. J. von Bardeleben, Solid State Commun. **57**, 137 (1986).